

# Motion-Coupled Sensing: When the State Change Powers Its Own Sensing

Muhammad Tahir, Muhammad Mubbashar Baig, Umer Irfan, Muhammad Ahad, Naveed Anwar Bhatti  
Department of Computer Science, Lahore University of Management Sciences (LUMS), Lahore, Pakistan  
{24030017, baig.muhammad, 27100363, 22260007, naveed.bhatti}@lums.edu.pk

**Abstract**—Batteryless IoT systems have largely followed two paths: ambient-energy sensing, where energy arrival is decoupled from the event being monitored, and kinetic event telegrams, where a user actuation powers a short report of the actuation itself. Mechanically gated states expose a third case: the access motion is not only an event to report, but the moment at which a latent physical state may have changed and must be measured. We show that routine hinge motion can supply enough energy for one bounded wake-sense-transmit transaction, including ultrasonic sensing and a long-range LoRa uplink. We call this principle *motion-coupled sensing* and instantiate it with an open-source compact electromagnetic harvester that retrofits to bins, doors, and cabinets with no structural modification. We size the platform for the most demanding workload, waste-bin monitoring, where each actuation must power both an ultrasonic measurement and a long-range LoRa uplink. Across five campus locations and 5,945 lid actuations, the bin deployment achieves 99.3% per-event transmission reliability. Field deployments on room doors with 1,870 actuations and office cabinets with 1,636 actuations achieve 92% and 94% transmission success respectively, demonstrating that the same energy envelope transfers across hinge geometries without hardware redesign. These results show that mechanical access can be treated as a self-powered sensing transaction, removing periodic polling and scheduled battery maintenance for IoT deployments.

## I. INTRODUCTION

Many IoT deployments monitor physical states that can change only through a mechanical action. A waste bin’s fill level changes when its lid opens; a room is entered when its door swings; a cabinet is accessed when its hinge moves. For such mechanically gated states, battery-powered periodic polling is structurally inefficient: the device spends energy checking for changes that are physically impossible between access events. This inefficiency compounds the operational burden of replacement schedules, silent node failures, and battery disposal [1], [2]. Solar harvesting can reduce this burden outdoors, but it remains unreliable for sensors installed indoors, in shaded areas, or inside enclosed objects [3].

This paper treats mechanical access not as a nuisance to be monitored, but as an energy source to be exploited. The same action that changes the monitored state releases a short burst of kinetic energy. If that energy can be captured and conditioned, it can power the full wake-sense-transmit pipeline: the node harvests energy from the access, wakes its electronics, senses or encodes the event, transmits a packet, and returns to zero idle current. We call this design pattern **motion-coupled sensing**: for mechanical-access objects, the motion that creates the information also triggers and powers the sensing transaction.

Conventional IoT nodes are optimized for long lifetime, duty cycling, or periodic sampling. A motion-coupled node is instead optimized for *per-event sufficiency*: each access event must provide enough usable energy to complete one bounded transaction. This removes scheduled battery maintenance and eliminates idle draw by leaving active electronics unpowered between access events.

Motion-coupled applications fall into two subclasses (Fig. 1c). In *event-only* applications, the access event itself is the information of interest; for example, a door or cabinet opening only needs to be encoded and reported. In *event-triggered sensing* applications, the access event supplies the trigger and energy, but the node must also measure a state affected by that access. Waste-bin monitoring is the canonical example: opening the lid is when the fill state may change, but the node must still measure the resulting fill level before transmission. This makes the bin variant the highest-energy workload because each actuation must power both active sensing and a long-range wireless uplink. The application is also practically important: poor solid waste management imposes significant public health burdens in developing regions [4], [5].

We present an open-source<sup>1</sup> batteryless platform built around a compact electromagnetic harvester that retrofits onto hinged access points without structural modification (Fig. 1a). A single actuation charges a capacitor, wakes a low-power MCU, performs sensing or event encoding, and transmits one LoRa packet. The active transaction completes in under 0.5 s, after which the node returns to zero idle current (Phases 4 and 5 in Fig. 1b). The same LoRa transceiver family supports both deployment regimes: spreading factor 10 (SF10) for outdoor long-range uplinks, and spreading factor 6 (SF6) for indoor short-range uplinks to nearby hubs.

The platform is sized based on measured access behavior. We instrumented waste bins with a rotary encoder and collected 832 lid interactions across five locations, measuring angular displacement, timing, and hinge-speed range. These measurements guided the generator selection and a 1:42.6 gear-train ratio, chosen to support the most demanding transaction: ultrasonic fill-level sensing plus a long-range LoRa uplink from one lid actuation. We evaluated the same platform across three hinged-access deployments. In outdoor waste-bin deployments, the platform achieves **99.3% per-event transmission reliability**

<sup>1</sup>Hardware designs, firmware, and analysis scripts are available at: <https://github.com/SYSNET-LUMS/Batteryless-event-driven-sensing-platform.git>

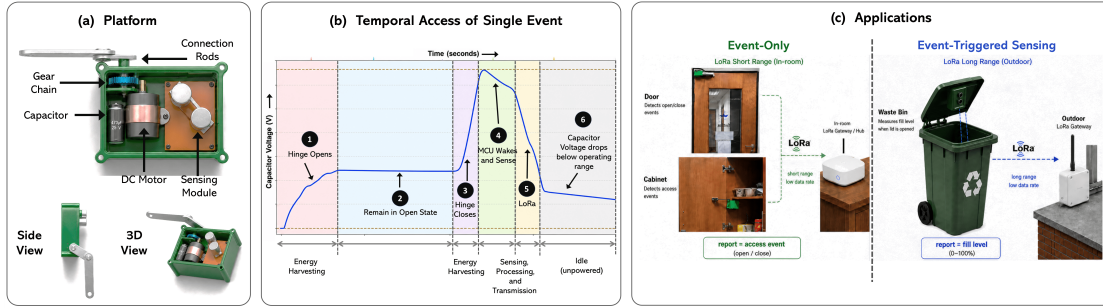


Fig. 1: Motion-coupled sensing as an atomic access transaction. (a) Platform retrofits to hinges such as bins, doors, and cabinets. (b) Access motion is not only an energy source; it also defines the state-validity boundary, wake-up trigger, and power source for the complete sense-and-send cycle. (c) Same hardware supports two subclasses: *event-only* reporting and *event-triggered sensing*.

over 5,945 lid actuations in three weeks. In indoor deployments, the same core achieves **92%** success over 1,870 room-door actuations and **94%** success over 1,636 cabinet actuations. These results show that a harvester sized for the highest-energy sensing workload transfers to lower-energy event-only monitoring across different hinge geometries at deployment scale.

### Contributions.

- [C1] **Mechanically gated sensing as a self-powered transaction.** We identify motion-coupled sensing as a class of IoT workloads where mechanical access defines the state-validity boundary, supplies the energy, triggers the node, and defines the reliability unit. Our event-triggered workload uses one access to power active sensing plus long-range LoRa reporting of the resulting state.
- [C2] **Transaction-sized harvester design.** We derive a reproducible batteryless harvester from 832 measured lid actuations across five campus sites, translating a 17.85–27.8 RPM hinge-speed envelope into a 1:42.6 gear train, 1000  $\mu\text{F}$  buffer, and 11.5 V wake-up threshold for a measured  $\sim 61$  mJ wake-sense-transmit transaction.
- [C3] **Field validation on the highest-energy workload.** We validate the platform on outdoor waste-bin sensing, the most demanding workload, across five campus locations and 5,945 lid actuations over three weeks, achieving **99.3% per-event transmission reliability**.
- [C4] **Multi-workload field validation across access types.** We field-deploy the same platform on room doors with 1,870 actuations and office cabinets with 1,636 actuations, achieving **92%** and **94%** per-event transmission success respectively without hardware redesign, demonstrating that the bin-sized energy envelope transfers across hinge geometries at deployment scale.

## II. RELATED WORK

### A. Smart Environments and Access Monitoring

Smart-bin systems commonly pair ultrasonic or infrared sensing with cellular, Wi-Fi, or LPWAN links to report fill level and schedule collections [6], [7]. Commercial systems extend lifetime with large batteries or solar/hybrid supply [8], [9],

while solar LoRaWAN smart-bin nodes show that batteryless waste monitoring is possible when outdoor light is available [3]. These designs reduce collection overhead, but they still treat sensing energy and bin access as separate concerns: the node is powered from a battery, solar source, or ambient harvester rather than from the lid motion that makes fill-level change possible.

Access monitoring in smart homes and buildings uses PIR sensors, reed switches, and BLE tags to detect occupancy or door/window state changes [10], [11]. Commercial kinetic building controls further show that a short human actuation can power a maintenance-free radio telegram [12]. Kinetic switches are the event-only endpoint of this design space: the actuation powers a short telegram reporting the actuation itself. Motion-coupled sensing targets the harder event-triggered case, where the access motion powers a post-access measurement of the physical state whose validity is bounded by that same access.

### B. Batteryless Communication and Intermittent Sensing

Battery-free RFID and backscatter platforms such as WISP and ambient backscatter demonstrate sensing and communication without batteries by harvesting or reflecting RF energy [13], [14]. Intermittent computing systems such as Mementos and Mayfly provide software support for long-running sensing tasks across repeated power failures [15], [16]. Batteryless LoRaWAN work has also modeled how capacitor-backed nodes should schedule sensing and transmission under scarce harvested energy [17]. These systems are important substrates for batteryless IoT, but they assume external RF, light, or other ambient energy and do not use the state-changing mechanical access event itself as the energy source, trigger, and transaction boundary.

### C. Kinetic and Event-Driven Harvesting

Kinetic energy harvesting has been explored with piezoelectric, electromagnetic, and rotational transducers for self-powered IoT systems [18], [19]. Event-driven harvesting nodes can recognize vibration events and transmit short alarms [20], and energy-neutral localization systems use motion-triggered operation to reduce idle cost [21]. These systems target ambient vibration, human motion, or localization updates rather than

TABLE I: Motion-coupled sensing relative to adjacent smart-sensing, batteryless, and kinetic systems.

System class	Energy model	Post-access sensing?	Range	Energy tied to access?
Battery smart-bin/access [6], [7], [10], [11]	stored battery	✓	long	✗
Solar batteryless bin [3], [8], [9]	ambient light	✓	long	✗
Kinetic event telegram [12]	actuation burst	✗	short	✓
RFID/backscatter [13], [14]	reader/RF field	limited	short	✗
Intermittent batteryless [15]–[17]	ambient	chunked	varies	✗
Event-driven kinetic [18]–[21]	motion	limited	short	no
<b>This work</b>	<b>access-motion burst</b>	✓	<b>SF10 long</b>	✓

mechanically gated object states. Motion-coupled sensing is therefore not generic kinetic harvesting: it uses kinetic energy only when that motion is causally tied to the state being monitored. In the bin workload, the access does more than announce itself; it powers the measurement that validates the resulting fill state. Table I summarizes the research gap this work is addressing.

### III. PLATFORM DESIGN

The platform implements the motion-coupled sensing transaction introduced in Section I. Each access event must satisfy three invariants: the motion must create or reveal the information of interest, the same motion must provide the energy burst to power the node, and the computation must be bounded so that one stored energy burst is sufficient to complete a wake–sense–transmit cycle. These invariants shift the design problem from continuous energy availability to *per-event sufficiency*. Unlike ambient harvesters, motion-coupled harvesting aligns energy arrival with moments when the monitored state can change. The design problem is therefore not long-term energy neutrality, but whether each access can provide enough energy for one bounded transaction. Rather than maintaining a node in a low-power polling state, the platform keeps active electronics unpowered until an access event has charged a local energy buffer above the threshold required for one reliable packet. Figure 1 summarizes the resulting architecture: a shared harvesting core captures hinge motion, while the sensing workload and radio configuration vary with the deployment.

#### A. Design Goals

Four goals guide the platform design.

- [D1] No scheduled battery maintenance:** Operate without primary or rechargeable batteries, eliminating replacement, recharging, and battery-aging failure modes.
- [D2] Retrofittable mechanical integration:** Attach to common hinged access points without permanent modification to the host object.
- [D3] Commodity, low-cost construction:** Use inexpensive and locally available parts, including DC motors as generators, spur gears, low-power microcontrollers, and off-the-shelf radios and sensors.
- [D4] Deployment-matched communication:** Use the same LoRa transceiver across deployments, with higher spread-

ing factors for outdoor long-range bins and lower spreading factors for short-range indoor doors and cabinets.

#### B. Platform Architecture

The system has three logical tiers. **(1)** At the edge, a batteryless node harvests kinetic energy from the access event and uses the stored burst to transmit either an access-event packet or a sensor measurement. **(2)** At the communication tier, packets are received by either an outdoor LoRaWAN gateway for long-range deployments or a nearby in-room LoRa hub for short-range deployments. **(3)** At the backend, packets are stored and optionally converted into alerts or downstream actions.

The central architectural choice is to keep the harvesting core shared across applications and vary only the application-specific front end. The shared core consists of the connecting-rod linkage, gear train, DC motor/generator, rectification and storage stage, and event-triggered power gate. The waste-bin variant adds an ultrasonic range sensor and uses long-range LoRa, while the door and cabinet variants omit the sensor and use short-range LoRa. This factoring allows one hardware platform to support both subclasses introduced in Section I: *event-only* applications, where the access event itself is the data, and *event-triggered sensing* applications, where the access event also powers a measurement.

#### C. Batteryless Edge Node

The edge node consists of four functional blocks: mechanical capture and amplification, electrical generation and storage, event-triggered power gating, and sensing-and-uplink.

1) *Mechanical Capture and Amplification:* A compact connecting-rod linkage transfers hinge motion to the harvesting core. This linkage converts opening and closing motion into rotation at the gear-train input (Section IV-C). A three-stage spur-gear train then amplifies the low hinge speed to the operating range of the generator. The final design uses a 1:42.6 ratio derived from the measured hinge-speed range and generator characterization.

2) *Electrical Generation and Storage:* The amplified rotation drives a 24 V DC motor used in generator mode. Because the generated voltage depends on hinge direction and speed, the motor output is rectified on a custom PCB. The rectified output charges a 1000  $\mu$ F, 25 V capacitor, which serves as the energy buffer for one access event. The capacitor feeds a buck converter that provides a regulated 3 V rail for the MCU, sensor, and LoRa radio. This regulation stage decouples the electronics from the time-varying generator output: the capacitor may charge to a higher voltage during harvesting, while the active electronics receive a stable supply during the wake–sense–transmit cycle. Once the capacitor voltage falls below the converter’s minimum input voltage ( $\approx 3$  V), the converter turns off; energy remaining below this point is unusable by the node. We use a capacitor rather than a rechargeable battery to support repeated charge–discharge cycles without scheduled replacement, consistent with **[D1]**. The complete power path, rectifier, storage capacitor, event-triggered power gate, and buck-regulated 3 V rail, is integrated on the custom PCB.

3) *Event-Triggered Power Gating*: A switch separates energy harvesting from computation and transmission. While the hinge is moving, the switch isolates the electronics so that harvested energy accumulates in the capacitor. Once the hinge reaches the triggering position, the switch connects the charged buffer to the regulator and microcontroller. This sequencing prevents the MCU and radio from drawing power before the buffer has reached a usable voltage. The trigger mechanism is deployment-specific. The bin variant uses a tilt switch actuated by lid closure. The door and cabinet variants use limit switches that can be placed at the fully closed position, fully open position, or both, depending on whether the application needs single or dual-event capture.

4) *Sensing and Uplink*: The work performed after wake-up depends on the application subclass. For event-only deployments, such as doors and cabinets, no sensor is required: the packet carries the node ID and event type, and the hub assigns the arrival timestamp. For event-triggered sensing, such as waste-bin monitoring, the MCU triggers an HC-SR04 ultrasonic sensor mounted inside the lid cavity and includes the fill-level reading in the uplink packet. Computation runs on a low-power ATmega328P [22] that boots only after the power gate closes. The radio configuration follows the deployment context [D4]. The bin variant uses an RA-02 LoRa module based on the SX1278 [23] at SF10 for outdoor long-range uplinks. The door and cabinet variants use the same module at SF6 for short-range indoor links to nearby hubs. SF6 is chosen for indoor use because the receiver is only meters away, the event-only payload is small, and the shorter time-on-air reduces transmission energy, leaving more margin for less predictable user-driven door and cabinet motions.

#### IV. HARVESTING SYSTEM DESIGN

The harvesting system is sized for one transaction rather than average power. In motion-coupled sensing, the central requirement is that a single access motion must charge the energy buffer enough to complete one wake-sense-transmit cycle. We size the system for the waste-bin variant because it is the highest-energy workload: each actuation must power ultrasonic sensing and a long-range SF10 LoRa uplink. Door and cabinet deployments are lower-energy event-only workloads, although their reliability depends on mounting geometry and user actuation behavior. The non-obvious challenge is that hinge speed (17.85–27.8 RPM) is far below the generator required speed, and the harvesting window ( $\sim 1.2$  s) is fixed by human behavior, neither parameter can be designed around, only matched. This section develops the sizing procedure. We first measure the energy required by one transaction, then characterize the hinge motion available during routine use. We use these measurements to select the generator, derive the gear ratio, and choose the capacitor based on required energy. We address following research questions in this work.

**Q1: How much energy does one long-range wake-sense-transmit cycle require?**

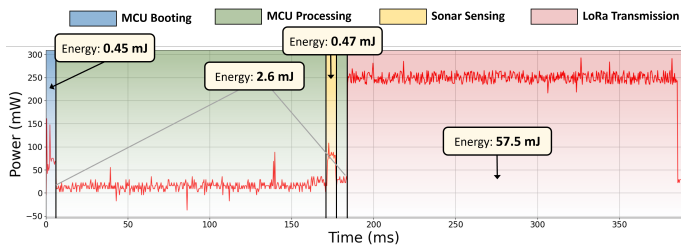


Fig. 2: Power waveform for single sensing-and-uplink cycle.

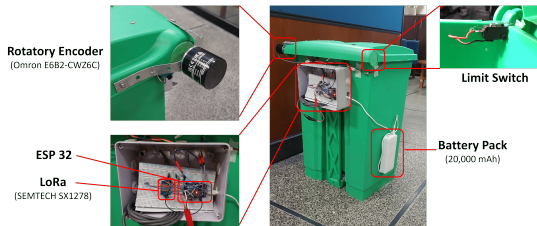


Fig. 3: Lid-motion instrumentation with encoder, limit switch, and ESP32 logging at millisecond resolution.

**Q2: Can routine hinge motion, captured with low-cost commodity hardware, supply this energy across observed access speeds?**

Q1 is answered through direct measurement of the node’s energy budget (Section IV-A). Q2 is addressed through hinge-motion characterization (Section IV-B) and drivetrain design (Section IV-C).

##### A. Per-Cycle Energy Budget (Q1)

We measured the bin variant in a lab configuration using an Arduino Pro Mini based on the ATmega328P, an HC-SR04 ultrasonic sensor, and an RA-02 LoRa module. The measurement captures the full active cycle: MCU boot, ultrasonic sensing, processing, and uplink. MCU startup consumes  $\approx 0.45$  mJ; ultrasonic sensing and processing consume  $\approx 3.0$  mJ; and LoRa transmission dominates at  $\approx 57.5$  mJ. The total measured energy for one bin transaction is therefore  $\approx 61$  mJ. Figure 2 shows the measured power waveform. The door and cabinet variants retain the same RA-02 LoRa radio but use SF6 instead of SF10, reducing packet airtime and transmission energy demand [24]. They also omit ultrasonic sensing. A harvester sized for the 61 mJ bin transaction therefore provides additional energy margin for these short-range event-only variants, motivating the asymmetric evaluation strategy used in Section VI.

##### B. Hinge-Motion Characterization (Q2)

To determine whether routine lid motion can supply the 61 mJ bin budget, we instrumented a 50-liter hinged-lid bin with an Omron E6B2-CWZ6C rotary encoder [25] and a limit switch at the fully closed position (Fig. 3). An ESP32 logged the encoder and switch signals at millisecond resolution and forwarded them via LoRaWAN for extraction of opening angle, opening duration, and closing duration.

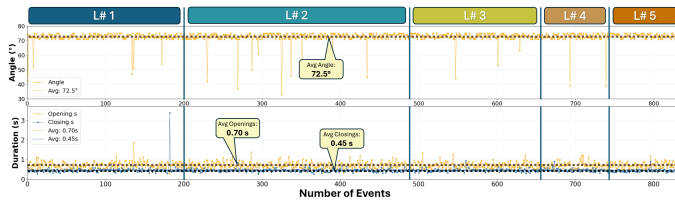


Fig. 4: Temporal and angular lid characteristics

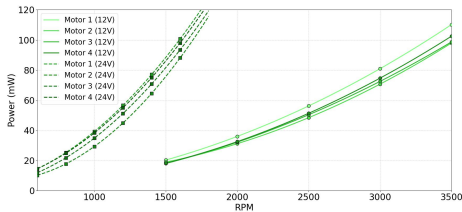


Fig. 5: Power vs. RPM for eight DC motors under  $470 \Omega$  load.

Across 832 lid interactions at five campus locations (Fig. 4), the mean opening angle was  $72.5^\circ$ , the mean opening duration was 0.70 s, and the mean closing duration was 0.45 s. Two findings drive the harvester design. First, closing is gravity-assisted and more repeatable than opening, making it the preferred trigger point for wake-up. Second, the observed hinge speeds, 17.85–27.8 RPM, are far below the operating range of a commodity DC motor used as a generator. The drivetrain must therefore amplify hinge speed before electrical generation.

### C. Generator Selection and Gear Train Design (Q2)

1) *Motor-as-Generator Characterization*: We evaluated eight commodity permanent-magnet DC motors of similar size ( $\approx 28$  mm diameter, 50 mm length): four rated at 12 V and four rated at 24 V. Each motor was tested on a variable-speed rig from 600 to 5000 RPM under a  $470 \Omega$  reference load, representing the average system load (Fig. 5).

To meet the 61 mJ bin budget, the generator must provide roughly 51 mW over the  $\approx 1.2$  s harvesting window formed by opening and closing. The 12 V motors reached this target only above 2200 RPM, requiring high mechanical amplification. The 24 V motors reached the same target at approximately 1100 RPM, reducing the required gear ratio by about half at the same volume price of \$1–1.5 per unit. We therefore select a 24 V DC motor for the harvester.

2) *Gear Ratio Design*: The required gear ratio follows from the measured hinge-speed range and the generator target. Mapping 17.85–27.8 RPM at the hinge to roughly 1100 RPM at the generator requires an amplification of about  $42.6\times$ . We implement this using a three-stage spur-gear train assembled from commodity parts: a 13-tooth motor pinion, two compound gears with 38-tooth outer and 13-tooth inner gears, and a 65-tooth driven gear:

$$13T \rightarrow 38T/13T \rightarrow 38T/13T \rightarrow 65T.$$

This train yields a 1:42.6 ratio, mapping the observed hinge-speed band to 760–1184 RPM at the generator. The lower end of this range is below the 1100 RPM nominal target, so slow or

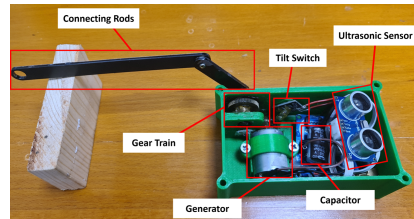


Fig. 6: Implementation of the harvesting module

partial actuations may not harvest enough energy for a complete transaction. In normal use, however, capacitor buffering and trigger-on-close sequencing allow full lid actuations to accumulate sufficient energy before wake-up. The field results in Section VI-A show that most full actuations cross the operating threshold, while the door and cabinet evaluations in Section VI show that the same ratio provides sufficient energy for lower-budget event-only workloads.

### D. Capacitor Sizing and Wake-Up Sequencing

Figure 6 shows the implemented mechanical assembly. The remaining design parameters are the storage capacitance and the wake-up threshold. We use a  $1000 \mu\text{F}$ , 25 V capacitor as the local energy buffer. The motor output is rectified on a custom PCB and used to charge the capacitor. A buck converter then regulates the capacitor voltage to a stable 3 V rail for the MCU, ultrasonic sensor, and LoRa radio. The converter operates only while its input voltage remains above its minimum. Once the capacitor falls below  $\approx 3$  V, the converter turns off, so energy stored below this voltage is unusable.

The usable energy in the capacitor is therefore the energy between the charged voltage and the converter cutoff:

$$E_{\text{usable}} = \frac{1}{2}C(V_{\text{charged}}^2 - V_{\text{cutoff}}^2).$$

With  $C = 1000 \mu\text{F}$ ,  $V_{\text{cutoff}} \approx 3$  V, and  $E_{\text{usable}} \approx 61$  mJ, the required charged voltage is

$$V_{\text{charged}} = \sqrt{\frac{2E_{\text{usable}}}{C} + V_{\text{cutoff}}^2} = \sqrt{\frac{2(61 \times 10^{-3})}{1000 \times 10^{-6}} + 3^2} \approx 11.45 \text{ V}.$$

We therefore use 11.5 V as the empirical minimum operating threshold for the bin variant. At this voltage, the  $1000 \mu\text{F}$  capacitor stores approximately 61.6 mJ of usable energy above the 3 V cutoff:

$$\frac{1}{2}(1000 \times 10^{-6})(11.5^2 - 3^2) \approx 61.6 \text{ mJ}.$$

The 25 V capacitor rating provides voltage headroom, while the selected capacitance is large enough to support LoRa peak current without excessive rail droop and small enough to recharge within one access event. Wake-up sequencing uses the closing asymmetry observed in Section IV-B. Because closing is gravity-assisted and more consistent across users, the bin variant triggers on lid closure. The tilt switch for bins, or limit switch for doors and cabinets, connects the charged capacitor to the regulator only after the hinge reaches its triggering position. This prevents the MCU and radio from drawing energy during harvesting. Once powered, the electronics complete the active transaction in under 0.5 s and then return to zero idle current.

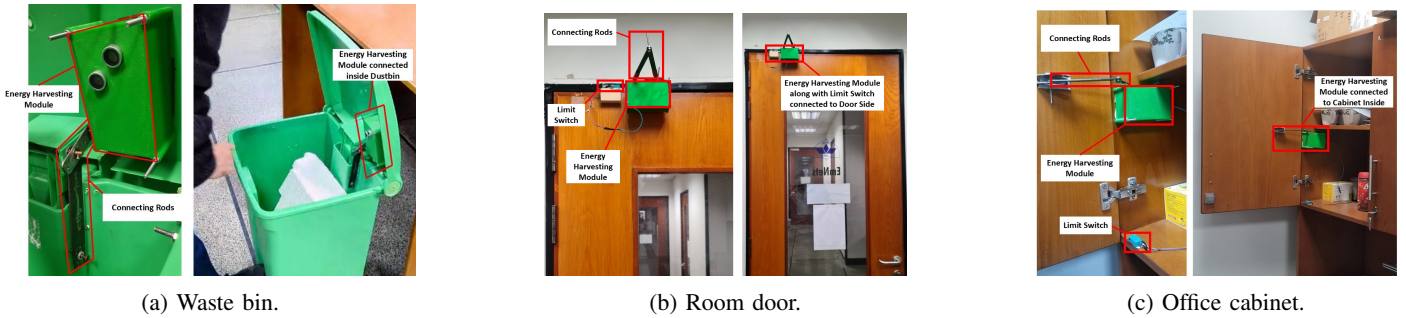


Fig. 7: Three deployments sharing the same harvesting core and RA-02 LoRa module.

## V. PLATFORM VARIANTS AND COST

We instantiate the platform in three hinged-access deployments using two electronics configurations. All variants share the same harvesting core and power path: mechanical assembly, rectifier, capacitor buffer, event-triggered power gate, buck-regulated 3 V supply, microcontroller, and RA-02 LoRa radio, as described in Sections III and IV. The variants differ only in sensing workload and radio configuration. The waste-bin variant adds ultrasonic sensing and uses long-range LoRa for outdoor uplinks; the door and cabinet variants omit sensing and use short-range LoRa to nearby indoor hubs.

### A. Waste Bin Lid (Event-Triggered Sensing)

The waste-bin module attaches inside the lid cavity of a standard 50-liter hinged-lid bin (Fig. 7a). An HC-SR04 ultrasonic sensor [26] faces downward from the top, maintaining acoustic line-of-sight to the waste surface while the enclosure protects the electronics and drivetrain from rain and debris. When the lid closes, a tilt switch connects the charged capacitor to the 3 V rail. The MCU triggers the sensor and transmits a long-range LoRa packet containing the node ID and fill-level reading. This variant targets outdoor campus and municipal deployments where the gateway may be hundreds of meters away.

### B. Room Door (Event-Only)

The door variant mounts the same harvesting core on the door frame near the hinge (Fig. 7b). Because the access event itself is the information of interest, no additional sensor is required. A limit switch at the fully closed rest position powers the node on door close, triggering a short-range LoRa packet containing the node ID and event type. The in-room hub assigns the arrival timestamp, so the batteryless node does not need to maintain a clock between events. Target applications include occupancy monitoring, energy-management triggers, and access logging in office or residential settings.

### C. Office/Home Cabinet (Event-Only)

The cabinet variant uses the same event-only configuration as the door variant, adapted to a smaller hinge geometry (Fig. 7c). A limit switch powers the node when the cabinet reaches the configured trigger position, and the node transmits a short-range LoRa packet containing the node ID and event type. As in the

TABLE II: BOM per Unit (USD, Volume  $\geq 1,000$  units)

Component	Long-Range Bin	Short-Range Door/Cabinet
MCU (ATmega328P)	1.50	1.50
LoRa Module (SX1278)	3.80	3.80
Ultrasonic Sensor (HC-SR04)	1.00	–
DC Motor/Generator (24 V)	1.50	1.50
Capacitor (1000 $\mu$ F, 25 V)	0.50	0.50
Power Management PCB	3.50	3.50
Gear Train (brass/plastic)	3.00	3.00
Connecting Rods	2.00	2.00
Enclosure (ABS plastic)	3.00	3.00
Limit/Tilt Switch	0.50	0.50
<b>Total BOM Cost</b>	<b>\$20.30</b>	<b>\$19.30</b>

door deployment, the in-room hub timestamps packet arrival. The field deployment in Section VI shows that the shared harvesting core provides sufficient energy for this lower-power event-only workload.

**Dual-event capture:** The cabinet variant can also support dwell-time logging by placing limit switches at both the fully open and fully closed positions. In this configuration, the opening motion powers and triggers an “opened” packet, while the closing motion powers and triggers a “closed” packet. The hub estimates dwell time from the arrival times of the two packets. This option adds one more switch and one more packet per access cycle, each powered by its corresponding hinge motion. Target applications include pharmaceutical compliance monitoring, office asset tracking, and smart-home appliance logging.

### D. Cost Analysis

Table II reports the per-unit BOM at volume pricing. The long-range bin variant costs \$20.30, while the short-range door/cabinet variant costs \$19.30. The \$1.00 difference is due only to the ultrasonic sensor; the harvesting core, MCU, radio, power management PCB, enclosure, and mechanical assembly are shared across all deployments. As a result, the platform supports multiple applications with a common supply chain and manufacturing process, while the BOM changes by only  $\approx 5\%$  between sensing and event-only configurations.

## VI. EVALUATION

Our evaluation follows the platform’s energy hierarchy. It does not ask whether a harvester can generate energy in isolation; it asks whether naturally occurring state-changing motions can complete one bounded sensing transaction with

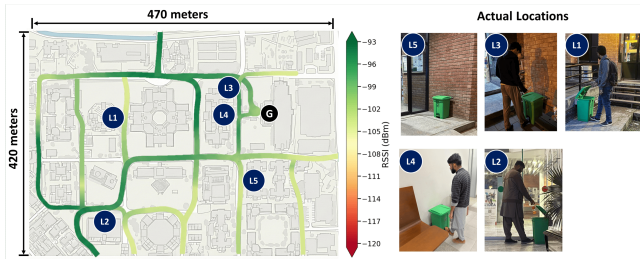


Fig. 8: Geographic distribution of bin deployment locations.

high per-event reliability. We first field-validate the highest-energy variant, waste-bin fill-level sensing, where each lid actuation must power both ultrasonic measurement and a long-range LoRa uplink. We then field-deploy the same harvesting core for door and cabinet event-only workloads at deployment scale (1,870 and 1,636 actuations respectively), testing whether the bin-sized energy envelope transfers across hinge geometries without hardware redesign. The three deployments together provide per-event reliability evidence across the full range of motion-coupled sensing workloads, from outdoor sensing-and-uplink to indoor event-only reporting.

#### A. Waste Bin: Full Field Validation

1) *Multi-Location Deployment*: We sequentially deployed the bin module at five moderate- to high-traffic campus locations (Fig. 8) under real outdoor conditions: 18–38°C temperature, 40–85% humidity, and occasional rainfall. The ultrasonic transducer faced downward inside the lid cavity, while the enclosure protected electronics and drivetrain from rain and debris [27], [28]. A rooftop LoRaWAN gateway received packets containing timestamp, bin ID, fill-level reading, and RSSI.

##### Deployment sites:

- Ⓒ **Gateway**: campus rooftop.
- Ⓘ<sub>1</sub> **Library**: consistent academic-hour traffic.
- Ⓘ<sub>2</sub> **Business School**: class-transition peaks.
- Ⓘ<sub>3</sub> **Cafe Entrance**: meal-time rapid successive actuations.
- Ⓘ<sub>4</sub> **Cafeteria**: traffic concentrated around meals.
- Ⓘ<sub>5</sub> **Dormitories**: Variable traffic with morning, evening peaks.

Because the system is event-driven, reliability is measured per access: one lid actuation should produce one complete sensing-and-uplink cycle. No periodic polling occurs between accesses; for a lidded bin, the last reported fill level remains valid until the next lid-opening event.

**Aggregate results**: Across all sites, the platform recorded **5,945 lid actuations** and **5,905 successful transmissions** over three weeks, achieving **99.3% per-event reliability** (Table III). Figure 9 shows packet outcomes and capacitor voltage over the deployment. The red dashed line marks the 11.5 V minimum transmission threshold. Most actuations produced exactly one packet; a few rapid re-openings produced two packets before the capacitor fully discharged.

**Packet distribution**: Of 5,945 lid actuations, 5,899 events (99.3%) produced exactly one packet. Six events (0.1%) pro-

TABLE III: Per-location bin deployment results.

Location	Actuations	Packets Sent	Success (%)
L1 Library	1,640	1,630	99.3
L2 Business School	918	913	99.4
L3 Cafe Entrance	1,514	1,506	99.4
L4 Cafeteria	607	604	99.5
L5 Dormitories	1,266	1,252	98.8
<b>Total/Avg</b>	<b>5,945</b>	<b>5,905</b>	<b>99.3</b>

duced two packets after rapid re-opening. Forty events produced no packet: 28 partial actuations (0.5%) did not charge the capacitor above 11.5 V, and 12 events (0.2%) were attributed to LoRaWAN channel loss. Post-deployment inspection showed no water ingress, minimal dust accumulation, and no visible corrosion or mechanical degradation across the five locations [D1][D2].

2) *Ultrasonic Fill-Level Accuracy*: Transmission reliability shows that one access event can power sensing and communication; the bin variant must also report a useful fill-level estimate. We therefore evaluate ultrasonic accuracy against depth-camera ground truth to separate sensing error from communication loss.

We mounted an Intel RealSense depth camera above a retrofitted bin and recorded 50 trials across varying waste configurations (Fig. 10), spanning the full bin depth range to expose any distance-dependent spread in ultrasonic readings. For each trial the walls were masked from the raw depth map to isolate the bin interior, and the masked values spatially averaged to produce a ground-truth fill level estimate. To mitigate setup misalignments, ultrasonic readings were adjusted for linear scaling and bias offset prior to comparison against the ground truth.

The HC-SR04’s  $\approx 15^\circ$  acoustic cone reports the dominant reflection within its sensing region rather than a point measurement. It therefore behaves as a coarse surface estimator: accurate when waste is distributed within the cone, but biased by protruding objects directly beneath the sensor. Across 50 trials, the system achieves a mean absolute error of 19.08 mm (Fig. 11), sufficient for coarse bulk fill-level estimation while identifying protrusions as the dominant failure mode.

**Operational interpretation**. Collection scheduling typically acts on coarse fill categories, such as *empty*, *quarter*, *half*, *three-quarter*, and *full*, rather than on millimeter-level fill curves [3]. For the bin’s 500 mm usable depth, these five categories correspond to roughly 100 mm per bucket, so an MAE meaningfully below this threshold suffices for collection routing. The error tail is dominated by a known geometric failure mode, a tall protrusion within the acoustic cone, which can be addressed through firmware or packaging refinements, such as multi-ping median filtering or a small acoustic baffle, and is orthogonal to the paper’s energy-harvesting contribution.

3) *Communication Range*: LoRa SF10 range was characterized at the deployment site (125 kHz BW, CR 4/8, 20 dBm, 8-symbol preamble, CRC); all five bin locations operated within the SX1278 link budget [23], [29], with RSSI degraded by foliage and building obstruction as expected.

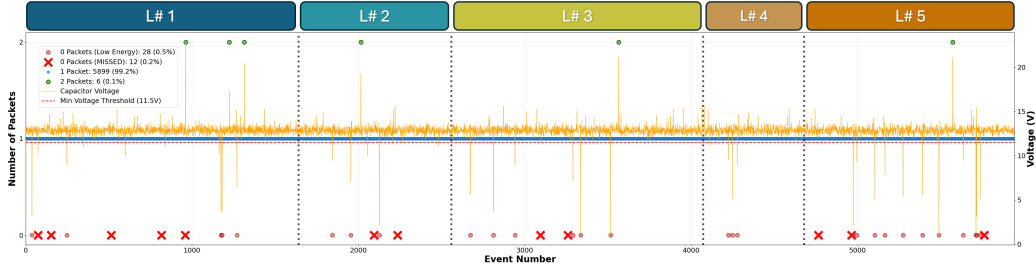


Fig. 9: Packet transmissions and capacitor voltage over 5,945 bin actuations.

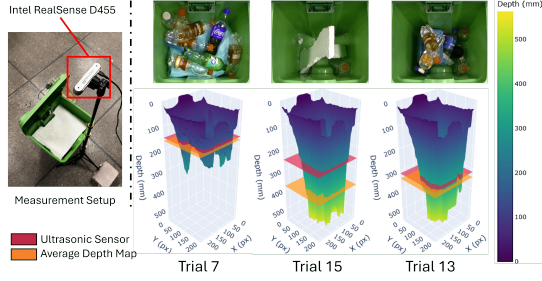


Fig. 10: Comparison of depth-camera and ultrasonic fill-level.

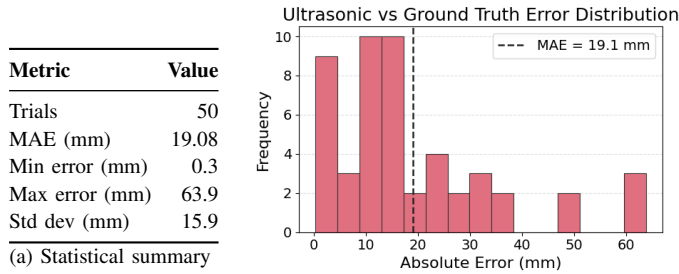


Fig. 11: Ultrasonic fill-level accuracy: statistical summary (a) and absolute error distribution across 50 trials (b).

4) *Mechanical Stress Test*: We subjected the mechanical assembly to a 10,000-iteration accelerated life test using the stepper-motor-operated actuator in Figure 12. The module transmitted successfully after every actuation. Post-test inspection showed no visible gear tooth wear, connecting-rod fatigue, mechanical misalignment, or enclosure damage. The full 7 hour test was recorded with visible timestamps throughout [30].

### B. Room Door: Field Deployment

The connecting-rod module was mounted on a standard interior door hinge in a university office without modifying the door or frame. A short-range LoRa receiver was placed in the same room. We conducted **1,870 door actuations** under normal use conditions documented in the supplementary video [31].

**Result**: Table IV indicates 1,724 of 1,870 actuations produced a packet, yielding a **92% success rate**. Each packet contained node ID and event type; the hub assigned the arrival timestamp. Post-deployment inspection showed no wear or misalignment, and the module added negligible resistance to

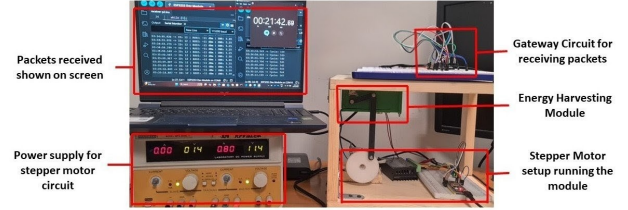


Fig. 12: Mechanical stress test setup

TABLE IV: Door and cabinet event-only field deployments.

Deployment	Actuations	Packets	Success	Dominant failure mode
Room door	1,870	1,724	92%	weak/partial closure
Cabinet	1,636	1,535	94%	variable user behaviour

door movement [D2]. At deployment scale, this confirms that the bin-sized energy envelope generalizes to a different hinge geometry without redesign, the same harvesting core powers reliable event-only reporting on a standard interior door with no battery, no ambient harvester, and no hardware modification.

### C. Office/Home Cabinet: Field Deployment

The cabinet trial used the same event-only hardware as the door variant. We conducted **1,636 cabinet actuations** under normal use conditions, documented in the supplementary video [32].

**Result**: Table IV indicates 1,535 of 1,636 actuations produced a packet, yielding a **94% success rate**. Packet contents and receiver configuration matched the door deployment. Post-deployment inspection showed no mechanical wear or alignment issues [D2]. This second deployment-scale evaluation confirms the energy budget transfers across a smaller hinge geometry: the same harvesting core powers reliable event-only reporting on a standard office cabinet without any hardware redesign relative to the bin or door variants.

## VII. DISCUSSION

### A. Scope of Motion-Coupled Sensing

Motion-coupled sensing targets IoT workloads where state changes are sparse, mechanically induced, and coupled to motion that can be harvested. It is therefore not a general replacement for battery-powered IoT, but a design pattern for access-gated sensing tasks. In this setting, the relevant reliability metric is not periodic uptime or battery lifetime, but

the probability that one access event produces one complete sensing transaction. This motivates our per-event reliability analysis across  $\sim 9,500$  actuations spanning three access types: bins, doors, and cabinets. The waste-bin variant defines the platform’s energy envelope because it combines ultrasonic sensing with long-range SF10 LoRa transmission, requiring approximately 61 mJ per cycle. Door and cabinet variants are lower-energy event-only workloads using short-range SF6 LoRa; their deployments confirm that the bin-sized energy envelope transfers across hinge geometries at scale. Motion-coupled sensing is not generic kinetic harvesting: it uses kinetic energy only when the motion is causally tied to the state being monitored. It is also distinct from event-driven sensing that assumes a separate power source and from intermittent computing that assumes scheduled energy arrival from external sources. Kinetic switches occupy the event-only endpoint; the harder case evaluated here is event-triggered sensing, where the same physical access both bounds the validity of the state and supplies the energy to measure and report that state.

### B. Limitations

The current prototype is limited to hinged access objects with sufficient angular displacement and a usable fixed anchor point for the connecting rod. Very small-displacement hinges, recessed hinges, sliding mechanisms, and objects without suitable mounting points are outside the present scope. While the three deployments establish per-event reliability at scale, longer studies are needed to evaluate weather exposure, and mechanical wear over months to years. Finally, the fill-level accuracy study validates coarse bulk estimation for one bin geometry; additional testing across bin shapes and waste profiles is needed before making application-specific accuracy claims.

## VIII. CONCLUSION

We introduced *motion-coupled sensing*, a design pattern for mechanically gated IoT workloads in which the access event creates the information, triggers the transaction, and supplies the energy needed to report it. We demonstrated this principle with an open-source batteryless platform built around a connecting-rod electromagnetic harvester, 1:42.6 gear train, 1000  $\mu\text{F}$  capacitor buffer, and event-triggered power gate. Sized for the highest-energy workload, the platform powers one wake–sense–transmit transaction per hinge actuation without scheduled battery maintenance. In outdoor waste-bin deployments, it achieves 99.3% per-event reliability over 5,945 lid actuations across five campus locations. Field deployments on indoor doors and cabinets extend this to lower-energy event-only workloads, achieving 92% success over 1,870 door actuations and 94% success over 1,636 cabinet actuations using the same harvesting core without redesign. These results show that mechanically gated sensing tasks can be treated as self-powered access transactions rather than periodically polled battery-powered workloads. For this class of IoT deployments,

the motion that changes the state can also serve as the trigger and energy source for sensing and communication.

## REFERENCES

- [1] J. Hester, “A battery free internet of things,” *Comm. of the ACM*, 2021.
- [2] D. Zhu and S. Beeby, “Kinetic energy harvesting,” *Energy Harvesting Systems: Principles, Modeling and Applications*, 2011.
- [3] S. Asenov and D. Tokmakov, “Using of batteryless LoRaWAN ultrasonic sensor node for smart garbage collection,” in *ELECTRONICA*, 2022.
- [4] A. K. Ziraba, T. N. Haregu, and B. Mberu, “A review and framework for understanding the potential impact of poor solid waste management on health in developing countries,” *Archives of Public Health*, 2016.
- [5] D. C. Wilson, C. A. Velis, and L. Rodic, “Integrated sustainable waste management in developing countries,” *Proceedings of the Institution of Civil Engineers: Waste and Resource Management*, 2013.
- [6] K. Pardini *et al.*, “IoT-based solid waste management solutions: A survey,” *Journal of Sensor and Actuator Networks*, 2019.
- [7] I. Sosunova and J. Porras, “IoT-enabled smart waste management systems for smart cities: A systematic review,” *IEEE Access*, 2022.
- [8] Nordsense, “Intelligent waste management solutions,” 2025.
- [9] Bigbelly, “Smart waste and recycling solutions,” 2025.
- [10] N. K. Suryadevara and S. C. Mukhopadhyay, “Wireless sensor network based home monitoring system for wellness determination of elderly,” *IEEE Sensors Journal*, 2012.
- [11] Kelly *et al.*, “Towards the implementation of IoT for environmental condition monitoring in homes,” *IEEE Sensors Journal*, 2013.
- [12] EnOcean GmbH, “EnOcean – the world of energy harvesting wireless technology,” White Paper, Feb. 2020.
- [13] A. P. Sample *et al.*, “Design of an RFID-based battery-free programmable sensing platform,” *IEEE TIM*, 2008.
- [14] V. Liu, A. Parks, V. Talla, S. Gollakota, D. Wetherall, and J. R. Smith, “Ambient backscatter: Wireless communication out of thin air,” in *Proceedings of the ACM SIGCOMM Conference*, 2013, pp. 39–50.
- [15] B. Ransford, J. Sorber, and K. Fu, “Mementos: System support for long-running computation on RFID-scale devices,” in *ASPLOS*, 2011.
- [16] J. Hester, L. Sitanayah, and J. Sorber, “Timely execution on intermittently powered batteryless sensors,” in *SenSys*, 2017.
- [17] A. Sabovic *et al.*, “Energy-aware sensing on battery-less LoRaWAN devices with energy harvesting,” *Electronics*, vol. 9, no. 6, p. 904, 2020.
- [18] Z. Chen, F. Gao, and J. Liang, “Kinetic energy harvesting based sensing and IoT systems: A review,” *Frontiers in Electronics*, 2022.
- [19] Y. Xu *et al.*, “Self-powered RPM sensor using a single-anchor variable reluctance energy harvester with pendulum effects,” in *ENSys*, 2023.
- [20] C. Liu *et al.*, “Design and implementation of an event-driven smart sensor node for wireless monitoring systems,” *Sensors*, 2023.
- [21] P. Mayer *et al.*, “Self-sustaining ultra-wideband positioning system for event-driven indoor localization,” *IEEE Internet of Things Journal*, 2023.
- [22] Atmel Corporation, “ATmega328P: 8-bit AVR microcontroller with 32k bytes in-system programmable flash,” Datasheet, 2015.
- [23] Semtech Corporation, “SX1278: 137 mhz to 1020 mhz low power long range transceiver,” Datasheet, 2015.
- [24] Saavedra *et al.*, “The smart meter challenge: Feasibility of autonomous indoor IoT devices depending on its energy harvesting source and IoT wireless technology,” *Sensors*, 2021.
- [25] Omron Corporation, “E6B2-CWZ6C incremental rotary encoder,” 2020.
- [26] ETC, “HC-SR04: Ultrasonic ranging module,” Datasheet, 2013.
- [27] I. Hong *et al.*, “IoT-based smart garbage system for efficient food waste management,” *The Scientific World Journal*, 2014.
- [28] D. Baldo *et al.*, “A multi-layer LoRaWAN infrastructure for smart waste management,” *Sensors*, 2021.
- [29] J. Petajarvi *et al.*, “On the coverage of LPWANs: Range evaluation and channel attenuation model for LoRa technology,” *ITST*, 2015.
- [30] “Batteryless harvester module: 10,000-iteration mechanical stress test (6 h 46 min),” <https://tinyurl.com/yn5ekxc2>, 2026.
- [31] “Batteryless harvester module: Door evaluation (2 h 25 min),” <https://shorturl.at/BA1z8>, 2026.
- [32] “Batteryless harvester module: Cabinet evaluation (1 h 13 min),” <https://shorturl.at/NqOQz>, 2026.